

Preparation and electrochemical properties of carbon-coated $\text{Li}_4\text{Ti}_5\text{O}_{12}$ anode materials for Lithium Ion Batteries

Er-Wei Zhang, Hai-Lang Zhang*

School of Chemical and Material Engineering, Jiangnan University,
Wuxi 214122, Jiangsu Province, P. R. China

*E-mail: zhl8868@vip.163.com

Received: 8 July 2018/ Accepted: 11 October 2018 / Published: 5 November 2018

$\text{Li}_4\text{Ti}_5\text{O}_{12}/\text{C}$ composites were synthesized by three different solid-state methods using polyvinyl alcohol (PVA) as a carbon source. The physical and electrochemical characteristics of pure $\text{Li}_4\text{Ti}_5\text{O}_{12}$ and $\text{Li}_4\text{Ti}_5\text{O}_{12}/\text{C}$ composites were extensively investigated. Comparing with $\text{Li}_4\text{Ti}_5\text{O}_{12}$ sample, the $\text{Li}_4\text{Ti}_5\text{O}_{12}/\text{C}$ composites show better electrochemical properties, especially for the discharge capacity and rate performance. Owing to the existence of conductive carbon layer, the reversible discharge capacities of $\text{Li}_4\text{Ti}_5\text{O}_{12}/\text{C}$ composites may go up to 175.5 mAhg^{-1} , and the capacity retention for the best system could reaches to 97.4% after 50 cycles. In addition, one of these composites shows excellent high rate discharge performance, the discharge capacity remains at 162.2 mAhg^{-1} at 3 C rate.

Keywords: Lithium-ion battery; Anode material; $\text{Li}_4\text{Ti}_5\text{O}_{12}$; carbon coating; PVA

1. INTRODUCTION

In recent years, more and more car-makers and high-tech companies have been working to develop the next generation electric vehicles such as electric vehicles (EVs) and plug-in hybrid electric vehicles (PHEVs) [1]. Rechargeable Li-ion batteries (LIBs), as the most key techniques for developing electric vehicles, attract concerns from both academic and industrial fields. Among several anode materials, due to unique properties, spinel $\text{Li}_4\text{Ti}_5\text{O}_{12}$ (LTO) has attracted widespread attention in lithium-ion battery industry and is regarded as one of the most possible substitutes for commercial graphite anode materials [2,3]. $\text{Li}_4\text{Ti}_5\text{O}_{12}$ shows superior cycle stability and outstanding reversibility during the charge-discharge process as a kind of "zero strain" material [4]. Furthermore, it possesses a flat voltage plateau at approximately 1.55 V (vs. Li^+/Li), which is higher than the reduction potential of most organic electrolytes ($\sim 0.8 \text{ V}$), thus avoiding the formation of a solid electrolyte interface (SEI) [5].

Unfortunately, the LTO has been found to have the problems of poor high-rate charge/discharge capabilities [6,7], and compared with some other anode materials, the volumetric capacity of LTO is still

low. The main reasons for its poor rate capability are its intrinsic low electronic conductivity (ca. 10^{-13} S·cm⁻¹) and moderate Li⁺ ion diffusion coefficient (10^{-8} cm²·s⁻¹), which could result in the serious polarization of the electrode when operated at high current densities [1]. Several effective ways have been utilized to improve the electrochemical performances of LTO, such as doping Al³⁺[8], Zn²⁺[9] in Li and Ti sites, synthesizing nano-Li₄Ti₅O₁₂ via various methods, and be coated with conductive materials such as Ag [10] and C [11]. After extensive research, it was proved that by using the method of surface coating of carbon layer, the electrochemical performances of LTO were significantly improved[1]. Owing to its excellent conductivity, a conducting carbonaceous material could be a best material to overcome the deficiency of LTO. Studies have shown that citric acid, polyacrylate acid and polyvinyl alcohol (PVA) [12] are all good choices to be used as carbon sources. Considering the efficiency and application economy, we use one of commonly used organic polymers (PVA) as carbon source in this study. Furthermore, among various methods to synthesize Li₄Ti₅O₁₂/C (LTO/C) composites, the solid-state sintering method has a simple and cost-effective synthetic route and more suitable for industrial production.

In this paper we synthesized the LTO/C composites by three different solid-state reaction methods and through analysis it can be concluded that the LTO/C prepared by a post-coating route showed the best electrochemical performances.

2. EXPERIMENTAL

2.1. Preparation of LTO and LTO/C composites

Li₄Ti₅O₁₂ and Li₄Ti₅O₁₂/C composites were prepared as following. The raw materials (TiO₂ (99.8%) and Li₂CO₃ (99.5%)) were mixed at the condition of the molar ratio of Li:Ti=4.2:5, and then were ball-milled to form slurry at the presence of ethanol as a dispersant. The above mixtures were dried and then sintered at 500 °C for 4 h in a flowing air atmosphere; the resulting precursor was pulverized to fine powders and annealed at 800 °C for 6 h under air atmosphere to obtain the homogeneous LTO sample.

The synthesis of LTO/C composites was similar to that of LTO sample, but using PVA as carbon source mixing with the raw materials in distilled water. PVA solution was mixed with as-prepared LTO (1:10 by weight) and was stirred for 0.5 h, and dried at 80 °C for 12 h to form dried powder, and then further was sintered at 700 °C for 1.5 h to obtain the post-coated material LTO/C-a.

The carbon coated TiO₂/C composite was also obtained by using PVA as carbon source and prepared via the similar carbon coating treatment as LTO/C-a. Then, final product LTO/C-b was prepared from Li₂CO₃ and TiO₂/C by one-step solid-state reaction (800 °C, 10 h). Furthermore, the LTO/C-c composite was obtained simultaneously by the reaction of Li₂CO₃ and TiO₂. According to the percentage mentioned above, PVA solution, Li₂CO₃ and TiO₂ were mixed together, followed by heat treatment in the same condition as LTO/C-b.

2.2. Electrode preparation and performance evaluation

The morphology of the synthesized LTO and LTO/C materials were analyzed by field emitting scanning electron microscopy (SEM, S4800). The crystal structures of the samples were analyzed by X-ray powder diffraction (XRD) with a Bruker D8 (made in Germany) with Cu K α radiation at scanning rate of 4° min⁻¹, and the diffraction patterns were recorded in the angle (2 θ) range from 10° to 90°. Cyclic voltammetry tests (CVs) were recorded from 1 V to 3 V with a scan rate of 0.2 mV·s⁻¹ by ZAHNER IM6 electrochemical workstation. The electrochemical impedance spectroscopy (EIS) measurement was also recorded using the same electrochemical workstation in the frequency range from 0.1 Hz to 100 kHz with perturbation signal amplitude of 5 mV.

Electrochemical performances of the LTO and LTO/C composites were measured with CR2032 coin cells, for which a lithium metal foil as the counter electrode and a Celgard 2325 porous polypropylene film was used as the separator. The electrolyte was consist of a solution of 1 M LiPF₆ in EC and DEC (1:1 by volume). The LTO/C and LTO working electrodes were prepared by mixing active materials, acetylene black and polyvinylidenetetrafluoroethylene (PVDF) binder in a weight ratio of 80:12:8, with N-methyl-2-pyrrolidone(NMP) as solvent and then pasted uniformly onto a copper foil and dried at 80 °C for 12 h in a vacuum oven. Finally, the cells were assembled in an argon-filled dry glove box (SUPER 1220/750, Made in China) and electrochemical performances were evaluated using Land battery test system (LAND CT2001A) at the cut-off voltages of 1–3 V under different current densities.

3. RESULTS

3.1. Material characterization

The X-ray diffraction patterns of the as-prepared LTO/C composites with various solid-state methods (LTO/C-a, LTO/C-b, LTO/C-c) are shown in Fig. 1. For comparison, the XRD pattern of the as-prepared LTO sample and the standard pattern of LTO (JCPDS card No. 49-0207) are shown in the bottom of the figure. As shown in the figure, the major peaks for all the samples are similar and correspond with the standard diffraction peaks, which indicates that the addition of carbon source PVA has no influence on the LTO phase. Furthermore, it can be clearly detected that the strength of diffraction peaks of LTO/C composites are increased in comparison with the LTO samples. The results indicate that LTO/C composites probably have larger crystallite sizes and this change can be attributed to that a certain thickness of carbon layer is formed on the surface of the LTO material.

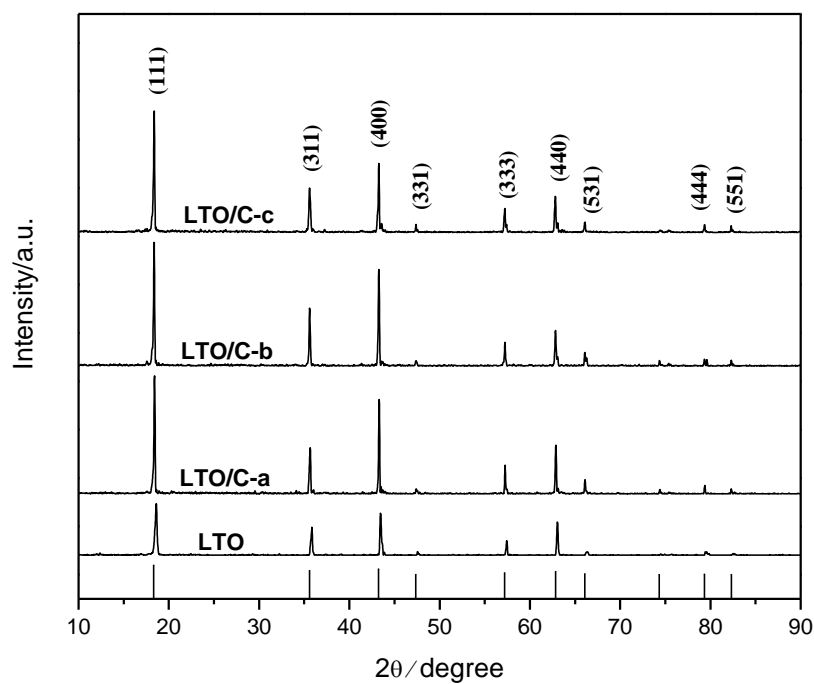


Figure 1. XRD patterns of the LTO and LTO/C samples LTO-a, LTO-b, and LTO-c.

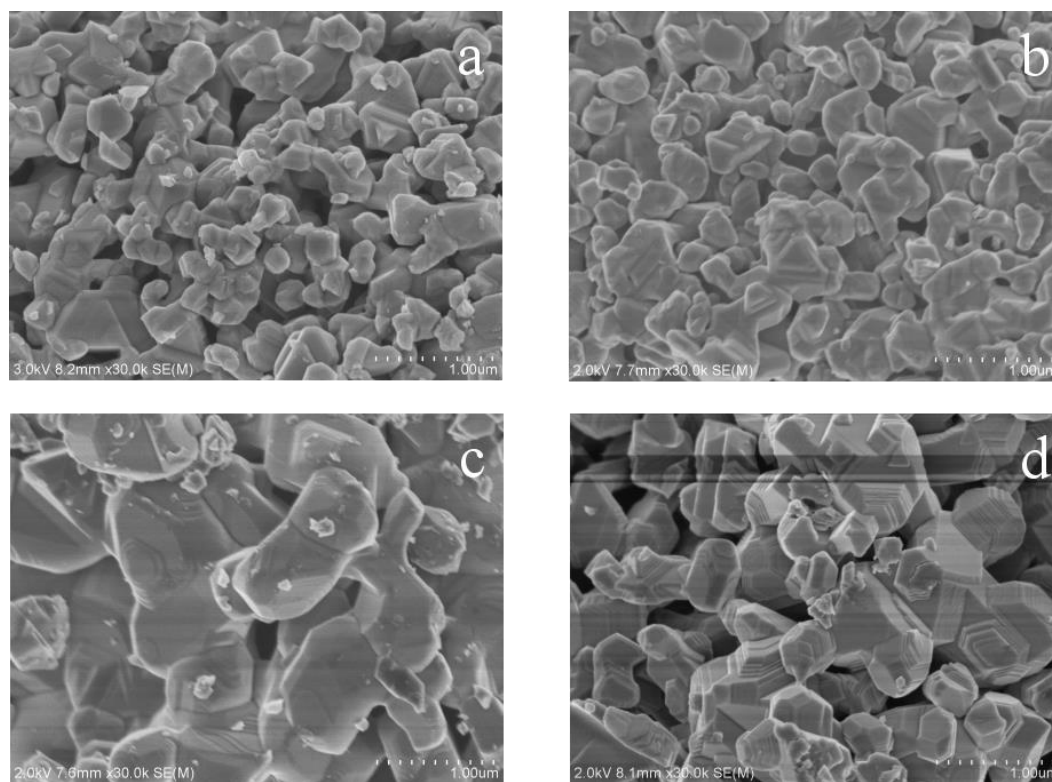


Figure 2. SEM images of (a) LTO and (b) LTO/C-a, (c) LTO/C-b, (d) LTO/C-c.

The scanning electron microscopy (SEM) for pure LTO and LTO/C composites (LTO/C-a, LTO/C-b and LTO/C-c) are shown in Fig.2. Clearly, LTO sample displays homogeneous size distribution and a narrow particle size of 100–300 nm. Whereas the LTO/C composites have a large number of amorphous particles with little agglomeration, which is consistent with the results of XRD patterns. Additionally, the reunion phenomenon of the LTO/C sample can be explained by the reason that a large number of amorphous particles from the carbonization of PVA form on the LTO surface [1,13]. By comparison of the Fig. 2b, c and d, the LTO/C-a sample exhibits better crystallinity with uniform and narrow size distribution, resulting in short lithium ion diffusion path and enough contact between the active material and electrolyte [14].

3.2. Electrochemical performance

In order to further demonstrate the effect of the carbon coating, the rate capability of the LTO/C composite are investigated and compared with LTO sample. Fig.3. shows the first charge–discharge curves of the pure LTO and LTO/C composites at 0.1C ($1C=175 \text{ mAhg}^{-1}$) rate in the voltage range between 1.0 and 3.0 V vs. Li^+/Li . It can be observed that both samples display similar and flat charge and discharge plateaus at around 1.55 V and 1.61 V, respectively, which corresponds to the two phase equilibrium between $\text{Li}_4\text{Ti}_5\text{O}_{12}$ and $\text{Li}_7\text{Ti}_5\text{O}_{12}$ [15,16].

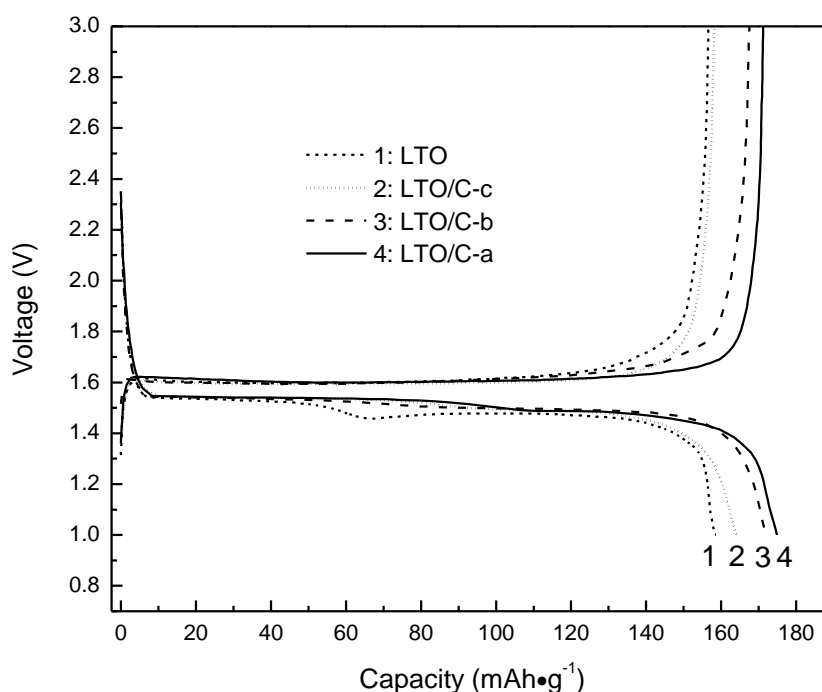


Figure 3. The first charge–discharge curves of LTO, LTO/C-a, LTO/C-b, and LTO/C-c samples at 0.1 C rate

Compared with pure LTO sample with a discharge capacity of 158.9 mAhg^{-1} , the discharge capacities of the carbon-coated LTO composites LTO/C-a, LTO/C-b, and LTO/C-c have been noticeably

improved, with the initial discharge capacity of 175.5 mAhg⁻¹, 173.1 mAhg⁻¹ and 166.9 mAhg⁻¹, respectively. Herein, it can be easily found LTO/C-a with a larger specific surface area and porous carbon layer possesses strong lithium storage capability compared to LTO/C-b and LTO/C-c.

Fig. 4 shows the cycle performance curves of the LTO and LTO/C anodes at a discharge rate of 0.2C, the initial and final 5 cycles are both at 0.1C. As shown in Fig. 4, an initial discharge capacity of the LTO/C-a composite is up to 175.5 mAhg⁻¹ and the capacity retention after 50 cycles is 97.4%. Table 1 shows the discharge capacities of first cycle and 50th cycle of the four samples and their capacity retention rates. Apparently, it can be concluded that the LTO/C-a composite prepared via the post-coating route has simultaneously higher discharge capacity and capacity retention for enhancing the lithium storage performance of LTO. To further study the rate capability for the LTO/C-a composite, a series of the discharge cycles for the as-prepared LTO and LTO/C samples were compared at various current rates between 0.1C and 3C, as shown in Fig. 5. It is clear that the discharge capacities of all samples gradually decrease with the increasing rates. This is because of that the utilization of the active material decreases as the rate increases [17]. When the rate increases from 0.1C to 3C, the discharge capacities of the four samples decrease to 124.1mAhg⁻¹, 162.2mAhg⁻¹, 151.1mAhg⁻¹ and 122.7mAhg⁻¹, respectively. It can be easily found that the LTO/C-a composite presents excellent high rate discharge capability and cycle stability among the three LTO/C materials. However, at the rate of 3C, LTO/C-c may even perform no better than the discharge capability of pure LTO sample. This may be due to that the carbon layer has not coated the LTO particles continuously in the LTO/C-c material, which results in poor electron conduction and poor high rate discharge performance.

Table 1. The capacities and capacity retention rates of LTO and LTO/C samples at 0.2C rate.

Sample	discharge/mAh·g ⁻¹ first cycle	Discharge/mAh·g ⁻¹ after 50 cycles	Capacity retention/%
LTO	158.9	152.1	95.7
LTO/C-a	175.5	170.9	97.4
LTO/C-b	173.1	164.6	95.1
LTO/C-c	166.9	161.0	96.5

To further investigate the synergetic enhancement of transport kinetics, it is necessary to analyze the electrochemical properties of these composites. Fig. 6 shows the cyclic voltammograms (CVs) of the as-prepared LTO and LTO/C composites obtained at a scan rate of 0.2 mV·s⁻¹. As shown in the figure, all plots of LTO and LTO/C samples exhibit similar oxidation/reduction peaks, which indicates that the carbon coating does not affect the electrochemical reaction of the LTO [18]. However, the potential differences of LTO/C samples were significantly decreased compared with LTO. This result shows that introducing carbon coating can decrease LTO electrode polarization effectively. Furthermore, LTO/C-a sample have a smaller half-peak width and potential differences than other LTO/C samples. This can be attributed to their higher electric conductivity caused by better porous carbon layer via the post-coating route.

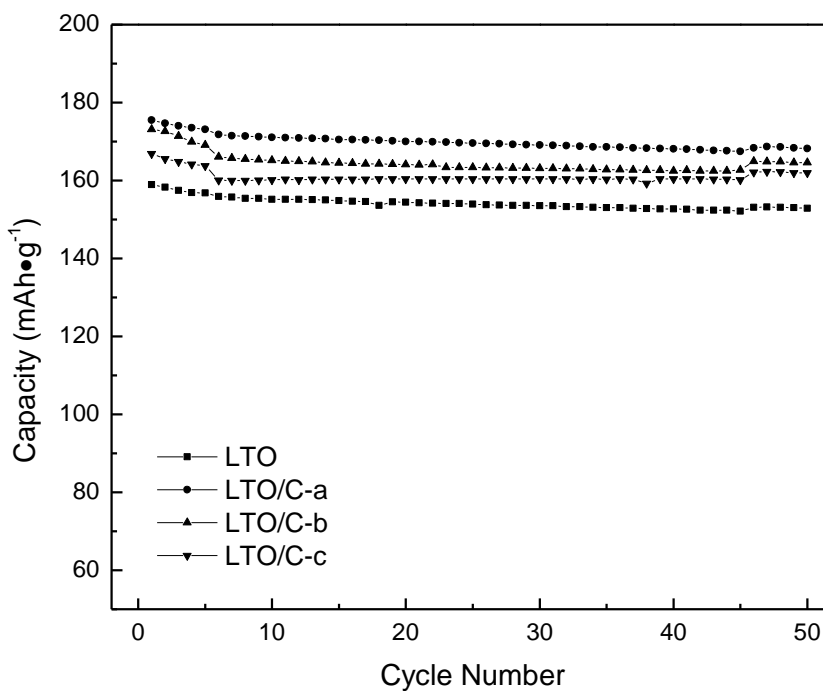


Figure 4. Cycling curves of as-prepared LTO and LTO/C , LTO/C –a, LTO/C –b and LTO/C –c at 0.2C.

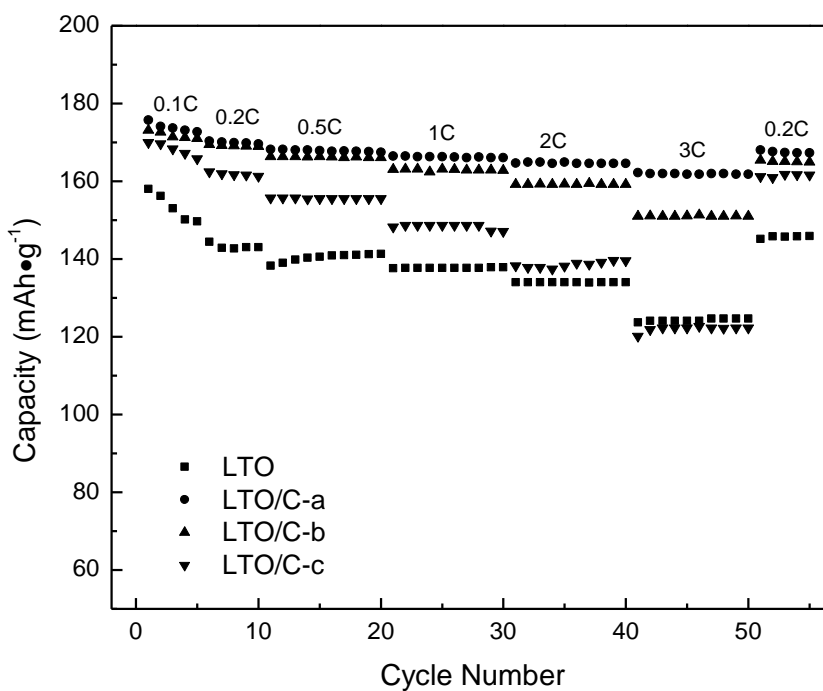


Figure 5. Rate capability tests of the LTO and LTO/C, LTO/C –a, LTO/C –b and LTO/C –c samples.

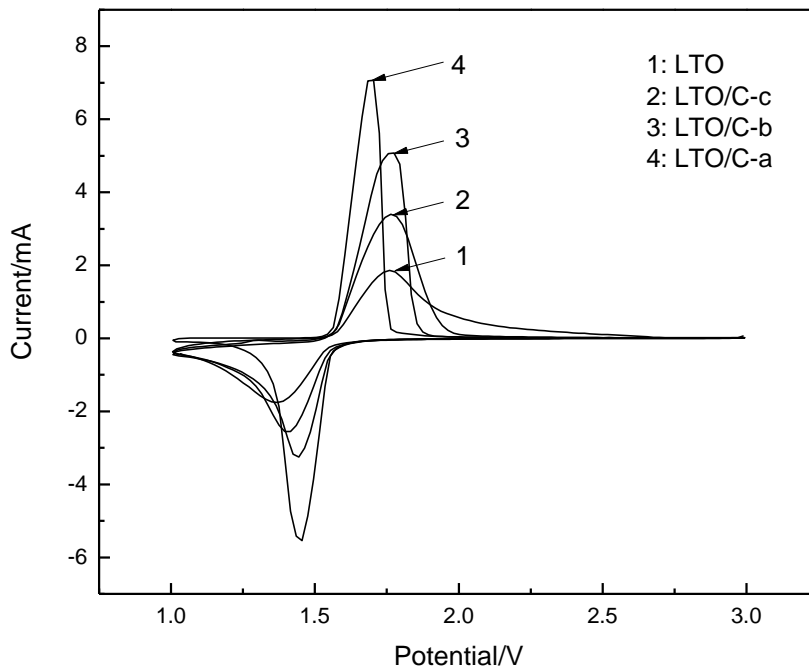
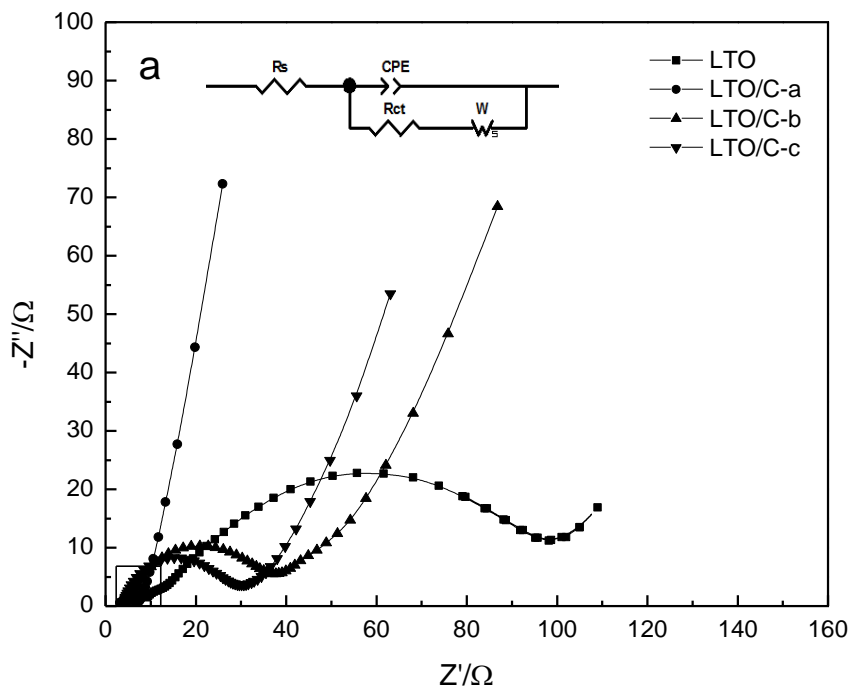


Figure 6. Cyclic voltammerty(CV) of LTO and LTO/C composites LTO/C –a, LTO/C –b and LTO/C –c.



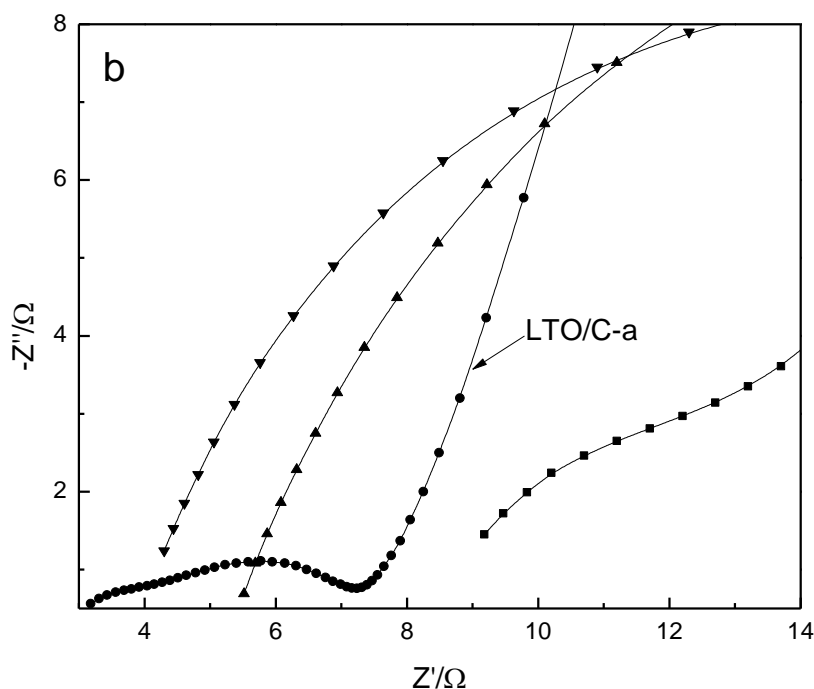


Figure 7. (a) Electrochemical impedance spectroscopy of pure LTO and LTO/C composite LTO/C –a, LTO/C –b and LTO/C –c.; the inset show the equivalent circuit used to fit the EIS; (b) The partial enlarged figure of fig7a.

Table 2. Impedance parameters of the LTO and LTO/C composites.

Samples	$R_s(\Omega)$	$R_{ct}(\Omega)$	Σ	$D_{Li}(cm^2s^{-1})$
LTO	9.473	105.8	20.19	6.83×10^{-12}
LTO/C-a	2.619	5.211	5.71	8.53×10^{-11}
LTO/C-b	5.11	31.37	15.01	1.23×10^{-11}
LTO/C-c	3.559	25.79	10.32	2.61×10^{-11}

Fig. 7a and b shows the corresponding Nyquist plots of the spectra, and the inset is the equivalent circuit used to simulate the obtained EIS spectra. It is obvious that each EIS spectrum is composed of a depressed semicircle and a straight line. According to literatures [19,20,21], R_s is the resistance of the electrolyte, R_{ct} the charge transfer resistance at the particle/electrolyte interface, and W is the Warburg impedance. The straight line in the low frequency is associated with lithium ion diffusion in $Li_4Ti_5O_{12}$ [22–24]. The lithium ion diffusion coefficient could be calculated from the low frequency plots according to the following equation [25–27]:

$$D_{Li} = R^2 T^2 / 2 A^2 n^4 F^4 C^2 \sigma^2 \quad (1)$$

Where R is the gas constant, T is the absolute temperature, A is the surface area of the cathode, n is the number of electrons per molecule during oxidation, F is the Faraday constant, C is the concentration of lithium ion. The value for σ can be calculated from the slope of the lines between Z' and $\omega^{-1/2}$, where ω is frequency. All the parameters obtained and calculated from EIS are summarized in

Table 2. The R_{ct} values of the LTO/C composites are remarkably lower compared to that of the LTO sample. The pronouncedly enhanced charge-transfer rate at the electrode/electrolyte interface can be attributed to the synergistic effect of the high conductive carbon layer and the mixed Ti^{3+} valance within the LTO/C, which both significantly enhance the electronic conductivity of LTO/C electrode [1]. Furthermore, LTO/C-a composite possesses the highest lithium diffusion coefficient (D_{Li}) compared with LTO/C-b and LTO/C-c. The large lithium diffusion coefficient shows that the LTO/C-a composite has better electrochemical performance including the high rate performance. Therefore, the post-coating route can effectively improve the electrical and ionic conductivities, lower the polarization of the electrode.

4. CONCLUSIONS

In summary, carbon-coated LTO was prepared by using PVA as carbon source through three simple and practical solid-state reactions. Characterization results show that all electrochemical performances of the LTO/C composites have been greatly improved due to the introduction of high conductive carbon layer. Through the comparison among the three methods, the LTO/C-a composite obtained through a post-coating route exhibits very good electrochemical properties such as high discharge capacity and good rate cycling performance. This may be by modifying the surface properties of sample or developing protection layers to reduce direct contact between electrolyte and active materials [28,29]. The superior performance is mainly attributable to the porous carbon layer, advanced electrode conductivity and narrow particle size of the LTO/C composite. With low cost and simple synthesis process, the LTO/C composite prepared though post-coating method could be a promising anode candidate material for high power lithium-ion batteries.

References

1. Y.C. Kuo, J.Y. Lin, *Electrochim. Acta*, 142 (2014) 43.
2. C. Lai, Y.Y. Dou, X. Li and X.P. Gao, *J. Power Sources*, 195 (2010) 3676.
3. J.Z. Chen, L. Yang, S.H. Fang and Y.F. Tang, *Electrochim. Acta*, 55 (2010) 6596.
4. T. Ohzuku, A. Ueda and N. Yamamoto, *J. Electrochem. Soc.*, 142 (1995) 1431.
5. C.M. Zhang, Y.Y. Zhang, J. Wang, D. Wang, D.N. He, and Y.Y. Xia, *J. Power Sources*, 236 (2013) 118.
6. B.H. Li, C.P. Han, Y.B. He, C. Yang, H.D. Du, Q.H. Yang and F.Y. Kang, *Energy Environ. Sci.*, 5 (2012) 9595.
7. L. Zhao, Y.S. Hu, H. Li, Z.X. Wang and L.Q. Chen, *Adv. Mater.*, 23 (2011) 1385.
8. J.Y. Lin, C.C. Hsu, H.P. Ho and S.H. Wu, *Electrochim. Acta*, 87 (2013) 126.
9. Z.W. Zhang, L.Y. Cao, J.F. Huang, S. Zhou, Y.C. Huang, and Y.J. Cai, *Ceram. Int.*, 39 (2013) 6139.
10. S.H. Huang, Z.Y. Wen, J.C. Zhang, Z.H. Gu and X.H. Xu, *Solid State Ionics*, 177 (2006) 851.
11. J. Gao, J. Ying, C. Jiang, and C. Wan, *J. Power Sources*, 166(2007) 255.
12. X.B. Hu, Z.J. Lin, K.R. Yang, Y.J. Huai and Z.H. Deng, *Electrochim. Acta*, 56 (2011) 5046.
13. L. Wang, Z. Zhang, G. Liang, X. Ou and Y. Xu, *Powder Technol.*, 79 (2012) 215.
14. Y.R. Ren, P. Lu, X.B. Huang, S.B. Zhou, Y.D. Chen, B.P. Liu, F.Q. Chu and J.N. Ding, *Solid State*

- Ionics*, 274 (2015) 83.
15. K.S. Park, A. Benayad, D.J. Kang and S.G. Doo, *J. Am. Chem. Soc.*, 130 (2008) 14930.
 16. Y.G. Wang, H.M. Liu, K.X. Wang, H. Eiji, Y.R. Wang and H.S. Zhou, *J. Mater. Chem.*, 19 (2009) 6789.
 17. X.H. Liu, Z.W. Zhao, *Powder Technol.*, 197 (2010) 309.
 18. X. Li, J. Xu, P.X. Huang, W. Yang, Z.Q. Wang and M.S. Wang, *Electrochim. Acta*, 190 (2016) 69.
 19. H. Liu, G. Wen, S. Bi and P. Gao, *Electrochim. Acta*, 171 (2015) 114.
 20. T. Yi, S. Yang, M. Tao, Y. Xie, Y. Zhu and R. Zhu, *Electrochim. Acta*, 134 (2014) 377.
 21. H. Liu, S. Bi, G. Wen, X. Teng, P. Gao, Z. Ni, Y. Zhu and F. Zhang, *J. Alloys Compd.*, 543 (2012) 99.
 22. L.M. Li, H.J. Guo, X.H. Li, Z.X. Wang, W.J. Peng, K.X. Xiang and X. Cao, *J. Power Sources*, 189 (2009) 45.
 23. H.Y. Wang, T.L. Hou, D. Sun, X.B. Huang, H.N. He, Y.G. Tang and Y.N. Liu, *J. Power Sources*, 247 (2014) 497.
 24. D. Sun, G.H. Jin, H.Y. Wang, P. Liu, Y. Ren, Y.F. Jiang, Y.G. Tang and X.B. Huang, *J. Mater. Chem.*, A 2 (2014) 12999.
 25. D. Sun, G.H. Jin, H.Y. Wang, X.B. Huang, Y. Ren, J.C. Jiang, H.N. He and Y.G. Tang, *J. Mater. Chem.*, A 2 (2014) 8009.
 26. A.Y. Shenouda, H.K. Liu, *J. Alloys Compd.*, 477 (2009) 498.
 27. A.Y. Shenouda, H.K. Liu, *J. Power Sources*, 185 (2008) 1386.
 28. H.Q. Li, H.S. Zhou, *Chem. Commun.*, 48 (2012) 1201.
 29. S.-H. Ng, J.Z. Wang, D. Wexler, K. Konstantinov, Z.-P. Guo, and H.-K. Liu, *Angew. Chem. Int. Ed.*, 45 (2006) 6896.

© 2018 The Authors. Published by ESG (www.electrochemsci.org). This article is an open access article distributed under the terms and conditions of the Creative Commons Attribution license (<http://creativecommons.org/licenses/by/4.0/>).